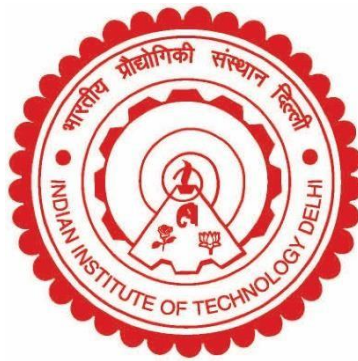


**ON THE PREDICTION OF PROPULSION OF A
PLUNGING RECTANGULAR PLATE**

NITIN KUMAR



**DEPARTMENT OF APPLIED MECHANICS
INDIAN INSTITUTE OF TECHNOLOGY DELHI
SEPTEMBER 2020**

©Indian Institute of Technology Delhi (IITD), New Delhi, 2020

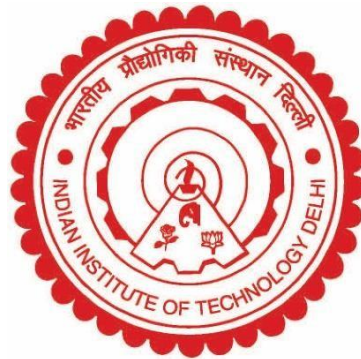
**ON THE PREDICTION OF PROPULSION OF A
PLUNGING RECTANGULAR PLATE**

by

NITIN KUMAR

DEPARTMENT OF APPLIED MECHANICS

Submitted in fulfilment of the requirements of the degree of doctor of
philosophy to the



INDIAN INSTITUTE OF TECHNOLOGY DELHI

SEPTEMBER 2020

Dedicated to my parents, Birbala and C.S.Baliyan.

CERTIFICATE

This is to certify that the thesis entitled “**ON THE PREDICTION OF PROPULSION OF A PLUNGING RECTANGULAR PLATE**” which is being submitted by **Mr. Nitin Kumar** in fulfilment of the requirement of the award of the degree of Doctor of Philosophy at Indian Institute of Technology Delhi is a bonafide work carried out by him under our supervision and guidance. The matter embodied in this thesis has not been submitted elsewhere for the award of any degree or diploma.

Dr. Sanjeev Sanghi

Professor

Department of Applied Mechanics

Indian Institute of Technology Delhi

New Delhi-110016

INDIA

Dr. Amit Gupta

Associate Professor

Department of Mechanical Engineering

Indian Institute of Technology Delhi

New Delhi-110016

INDIA

ACKNOWLEDGEMENTS

Finishing this dissertation is a matter of immense pleasure, satisfaction, and pride for me. It has been a long journey since I joined IIT Delhi and there are many people to whom I want to extend my gratitude who supported me in accomplishing this task.

I am profoundly grateful and indebted to my supervisors Prof. Sanjeev Sanghi and Dr. Amit Gupta for their invaluable guidance and unwavering encouragement throughout my doctorate. They willingly shared ideas and suggestions from their vault of experience at every instance of my stagnation and unpretentiously expressed their inability whenever the problem was beyond their horizon of knowledge. More than mentors, they have been like family members whom I could always approach without reluctance in the hour of need. Their long stimulating consultations always cheered me and revived enthusiasm whenever I was disheartened or surrounded by pessimistic thoughts. And at times, the dosage of their criticism ensured that I was redirected on track and eradicated any nascent complacency trying to conquer my mind.

I will be forever obliged to my parents and my wife for her support, advice and constant motivation which has been instrumental in completing this thesis. They were considerate enough to understand the nature of my work that often extended beyond the normal working hours and never complained about my negligence of responsibility towards my family.

I would also like to acknowledge the financial support received from my parent institute, i.e., G. B. Pant Institute of Engineering and Technology under TEQIP programme. I also thank the IIT Delhi high-performance computing (HPC) facility for computational resources on which numerical simulations were performed.

This dissertation would be incomplete without the special salutation to Dr. Nipun Arora for his thought-provoking propositions and ingenious discussions throughout my research.

I also extend my appreciation to my past and present lab members, Dr. Muhammad Rashid, Dr. Salahuddin Ahamad, and Dr. Rattandeep Singh for keeping the working atmosphere amicable that fostered brilliant ideas and helped me to steer through effortlessly.

Nitin Kumar

ABSTRACT

Recently, researchers and scholars have been engaged in a more profound examination of insect flight as it represents one of nature's best cases of species presented with amazing mobility and direction-finding abilities and that has motivated designers to plan micro air vehicles (MAVs) on a comparable idea. In any case, the aerial fluttering flight includes complex fluid-dynamical phenomena that do not follow the traditional quasi-steady hypotheses pervasive in fixed-wing optimal design. Moreover, the scientific understanding of how the instability of periodic flow associated with plunging wing effects the onset of propulsion is far from complete, especially with regard to the plunging frequency and amplitude of insect wings. Thus, in this study, a real plunging insect wing is mimicked by utilizing a fluid-structure interaction system. The aerodynamic forces on the plate are determined by an in-house fluid solver that utilizes a novel translating continuous-grid-block model using a multiple-relaxation time variant of the lattice Boltzmann method.

The key parameters expected to play a significant role in self-propulsion are the plunging Reynolds number (Re_f), plate thickness to chord ratio (δ), non-dimensional amplitude or Keulegan-Carpenter number (KC) and non-dimensional frequency or Stokes number (β). Numerical simulations are performed on a self-propelled plunging rectangular plate to understand the impact of these parameters on the breaking of symmetry that leads to the onset of propulsion. The non-dimensional trajectory of the centre of mass of the plate and flow structures associated with the plate on the asymmetry side in the proximity of the transition boundary in KC - β space are also examined.

The onset of asymmetry that leads to the propulsion of a self-propelled plunging plate in a quiescent fluid is predicted using Floquet analysis. This analysis utilizes a periodic base flow of initial plunging cycles obtained through the fluid solver. The governing equations for

Floquet analysis, discretized using the finite-difference method in two-dimensions, are subsequently written in the form of perturbed equations with two-dimensional disturbances. These equations are linearized around the base flow, which results in a set of partial differential equations that govern the evolution of the perturbations. The eigenvalues, stability of the periodic base flow and the points of bifurcations are resolved through the normal mode analysis.

Simulations show that the transition boundary in KC - β space shifts to smaller KC for given β as δ is reduced, suggesting that breaking of symmetry is motivated for a plate with lower δ . Furthermore, four distinct movement of non-dimensional coordinate of the center of mass of plate with respect to plunging cycles are identified. These movements are further differentiated with flow patterns associated with the plunging plate during propulsion and the frequency of coefficient of horizontal thrust. Finally, the effect of ground clearance (ζ) on the propulsion of the plate is investigated.

सार

हाल ही में, शोधकर्ताओं और विद्वानों ने कीट की उड़ान की अधिक गहन परीक्षा में भाग लिया है क्योंकि यह प्रकृति की सबसे अच्छी प्रजातियों में से एक है जो अद्भुत गतिशीलता और दिशा-खोज क्षमताओं के साथ प्रस्तुत की गई है और जिसने डिजाइनरों को सूक्ष्म वायु वाहनों (MAV) की योजना बनाने के लिए प्रेरित किया है। तुलनीय विचार। किसी भी मामले में, एरियल स्पंदन फ्लाईंग में जटिल तरल-गतिशील घटनाएं शामिल हैं जो फिक्स्ड-विंग इष्टतम डिजाइन में पारंपरिक अर्ध-स्थिर हाइपोथेसिस व्यापकता का पालन नहीं करती हैं। इसके अलावा, प्लंजिंग विंग के प्रभाव से जुड़ी आवधिक प्रवाह की अस्थिरता के बारे में वैज्ञानिक समझ, प्रणोदन की शुरुआत पूरी तरह से दूर है, विशेष रूप से कीटों की पंखों की प्लंबिंग आवृत्ति और आयाम के संबंध में। इस प्रकार, इस अध्ययन में, एक तरल पदार्थ-संरचना इंटरैक्शन सिस्टम का उपयोग करके एक वास्तविक प्लंजिंग कीट पंख की नकल की जाती है। प्लेट पर वायुगतिकीय बलों को एक इन-हाउस द्रव सॉल्वर द्वारा निर्धारित किया जाता है जो जाली-बोल्जमैन विधि के कई-विश्राम समय संस्करण का उपयोग करके निरंतर-ग्रिड-ब्लॉक मॉडल का अनुवाद करने वाले उपन्यास का उपयोग करता है।

आत्म-प्रणोदन में एक महत्वपूर्ण भूमिका निभाने के लिए अपेक्षित प्रमुख पैरामीटर हैं रेनॉल्ड्स संख्या (Re_f), प्लेट मोटाई से कॉर्ड अनुपात (δ), गैर-आयामी आयाम या Keulegan-Carpenter संख्या (KC) और गैर-आयामी आवृत्ति या स्टोक्स संख्या (β)। स्व-चालित प्लंबिंग आयताकार प्लेट पर संख्यात्मक सिमुलेशन प्रदर्शन किया जाता है ताकि समरूपता के टूटने पर इन मापदंडों के प्रभाव को समझा जा सके जो प्रणोदन की शुरुआत की ओर जाता है। प्लेट के द्रव्यमान के केंद्र के गैर-आयामी प्रक्षेपवक्र और KC - β अंतरिक्ष में संक्रमण सीमा की निकटता में विषमता पक्ष पर प्लेट से जुड़े प्रवाह संरचनाओं की भी जांच की जाती है।

असममितता की शुरुआत जो एक स्वैच्छिक द्रव में एक स्व-चालित प्लंजिंग प्लेट के प्रसार की ओर ले जाती है, फ्लोकेट विश्लेषण का उपयोग करके भविष्यवाणी की जाती है। यह विश्लेषण द्रव सॉल्वर के माध्यम से प्राप्त प्रारंभिक प्लंजिंग चक्रों के आवधिक आधार प्रवाह का उपयोग करता है। दो आयामों में परिमित-अंतर विधि का उपयोग कर विवेकाधीन फ्लोकेट विश्लेषण के लिए शासित समीकरण बाद में द्वि-आयामी गड़बड़ी के साथ गड़बड़ी समीकरणों के रूप में लिखे गए हैं। ये समीकरण आधार प्रवाह के चारों ओर रैखिक होते हैं, जिसके परिणामस्वरूप आंशिक अंतर समीकरणों का एक सेट होता है जो गड़बड़ी के विकास को नियंत्रित करते हैं। सामान्य मोड विश्लेषण के माध्यम से eigenvalues, आवधिक आधार प्रवाह की स्थिरता और द्विभाजन के बिंदुओं को हल किया जाता है।

सिमुलेशन से पता चलता है कि $KC-\beta$ अंतरिक्ष में संक्रमण सीमा दी गई δ के रूप में छोटे KC के लिए स्थानांतरित हो जाती है इसलिए यह सुझाव दिया गया है कि समरूपता को तोड़ना निचले δ के साथ एक प्लेट के लिए प्रेरित होता है। इसके अलावा, प्लंजिंग चक्रों के संबंध में प्लेट के द्रव्यमान के केंद्र के गैर-आयामी समन्वय के चार अलग-अलग आंदोलन की पहचान की जाती है। प्रणोदन के दौरान प्लंजिंग प्लेट से जुड़े प्रवाह पैटर्न और क्षैतिज जोर के गुणांक की आवृत्ति के साथ इन आंदोलनों को और विभेदित किया जाता है। अंत में, प्लेट के प्रणोदन पर ग्राउंड क्लियरेंस (ζ) के प्रभाव की जांच की जाती है।

Table of Contents

CERTIFICATE	i
ACKNOWLEDGEMENTS	iii
ABSTRACT.....	v
संक्षेप.....	vii
LIST OF FIGURES	xii
LIST OF TABLES	xvi
NOMENCLATURE.....	xvii
Chapter 1	1
INTRODUCTION	1
1.1 Background	1
1.1.1 Types of MAVs.....	2
1.1.2 Self-propelled wing.....	2
1.2 Motivation	3
1.3 Challenges and opportunities	4
1.4 Objectives.....	5
1.5 Outline of the thesis.....	6
Chapter 2	9
LITERATURE REVIEW.....	9

2.1 Early methodologies for demonstrating insect flight.....	9
2.2 Unsteady mechanisms in flapping aerodynamics	10
2.3 Thrust generation due to flapping oscillation	13
2.4 Linear stability analysis	21
2.5 Floquet analysis	23
2.4 Conclusions from the literature review	27
Chapter 3	29
METHODOLOGY.....	29
3.1 Flow solver.....	29
3.1.1 Boltzmann transport equation	29
3.1.2 Single-Relaxation Time Model.....	33
3.1.3 Multi-Relaxation Time Model	35
3.1.4 Boundary Treatments.....	39
3.1.5 Salient feature of LBM	41
3.2 Computational Domain.....	42
3.3 Stability analysis	43
3.3.1 Floquet analysis	43
3.3 Summary	48
Chapter 4	51
LINEAR STABILITY ANALYSIS OF TWO-DIMENSIONAL LAMINAR FLOWS	51
4.1 Uniform flow past a square cylinder.....	51

4.2 Double-glazing problem	57
4.3 Summary	62
Chapter 5	65
RIGID PLUNGING PLATE.....	65
5.1 Plunging kinematics and parameters	65
5.3 Numerical Simulations.....	68
5.3.1 Comparison with earlier studies.....	68
5.3.2 Hovering	71
5.3.3 Onset of propulsion or symmetry breaking for the plunging plate	72
5.4 Floquet analysis	76
5.5 Flow structure associated with a self-propelled plunging plate.....	80
5.6 Effect of ground clearance (ζ) on the propulsion of plate.....	86
5.7 Summary	88
Chapter 6	91
CONCLUSIONS.....	91
REFERENCES.....	97
APPENDIX	107
Publications International Journals	109
International Conferences	109
Bio-data of author	109

LIST OF FIGURES

Figure 1. Prototypical (MAVs): (a) fixed-wing MAV with a 15 cm wingspan [11], (b) rotary-wing MAV with 8.5 cm diameter design [12], and (c) flapping wing MAV [13].....2

Figure 2. (a) Numerical simulations carried out by Arora et al. [33] on two elliptical membranes acting ‘Clap and Fling’ proclaiming the rise in lift coefficient because of “wing-wake interaction” that ceases to exist at low Reynolds number. (b) During the ‘Clap and Fling’ movement, the fluid flows around wings used by small insects to overcome the Wagner effect. (c) (i) Von-Karman vortex and (ii) Inverted Von-Karman vortex along with the corresponding velocity profile. (d) A schematic representation of vortex dipoles reproduced from [34]. Circulation Γ can be determined by integrating the vorticity over the rectangular box considered around the vortex. 11

Figure 3. Change in a particle's position and velocity due to external force (recreated from [94]).....30

Figure 4. Lattice arrangement for the D2Q9 model.....34

Figure 5. The layout of the regularly spaced lattices and curved solid boundary (solid blue). The filled and hollow circles signify solid and fluid nodes individually. The solid squares denote the boundary nodes. The dotted line represents the halfway bounce back interpretation of the curved geometry.40

Figure 6. (a) Grid distribution around the plate; (b) Layout of the computational domain with imposed boundary conditions separated into various zones (by blue dash-dot lines) pick up by multi-processors.....43

Figure 7. Typical grid spacing diagram and the nomenclature for the distances used in Equations (3.60) and (3.61).46

Figure 8. The layout of the computational domain with the imposed boundary conditions. ...	53
Figure 9. Distribution of smallest eigenvalues for normal mode, at $Re = 51, 52$ and 53	55
Figure 10. The onset of vortex shedding at $Re = 52$	56
Figure 11. (a) vorticity and (b) stream function twenty evenly spaced contours between -0.60 (blue) and $+0.60$ (red) for the steady-state solution and the real and imaginary parts of the eigenvector at critical Reynolds number of 51	57
Figure 12. (a) Enclosure geometry and boundary conditions and (b) temperature boundary condition along the bottom and top walls of the square enclosure.	58
Figure 13. (a) Plots of the complex eigenvalues spectrum at four critical values of the Rayleigh number. Only eigenvalues with a positive imaginary part are shown. Dashed lines join eigenvalues computed at the same Rayleigh number (b) Comparison of results with Winters [84] at Rayleigh number of 2.04×10^6	61
Figure 14. (a) Stream function and (b) isotherm twenty evenly spaced contours between -0.025 (blue) and $+0.025$ (red) for the steady-state solution and the real and imaginary parts of the eigenvector at critical Rayleigh number of 1.88×10^6	62
Figure 15. Schematic representation of a self-propelled rigid plunging membrane.	66
Figure 16. A pictorial representation of plunging amplitude A	66
Figure 17. The geometry of an elliptical foil with ($\delta=0.1$) and comparison of location of transition boundaries in $KC-\beta$ expansion between the two-dimensional symmetrical and asymmetrical flow of present study with Deng and Caulfield [91].	69
Figure 18. A comparison of translational Reynolds number Re_u as a function of flapping Reynolds number Re_f between present study and Alben and Shelley[54] for an elliptical airfoil with $\rho^* = 32$, $KC = 3.14$ and $\delta = 0.1$	70
Figure 19. The fifteen evenly spaced vorticity contours between -0.30 (blue) and $+0.30$ (red) produced by a plunging plate at $KC = 3.8$ and $\beta = 1.67$. The accompanying figure on the right	

of each plot illustrates the instantaneous positions and the direction during one cycle. Red and blue colors demonstrate anticlockwise and clockwise rotation, respectively..... 71

Figure 20. Variation of flow transition boundaries characterizing possibility of horizontal motion in KC - β space and in Re_f - β space for $\delta = 0.1$ 73

Figure 21. Fifteen evenly spaced time intervals vorticity contours between -0.40 (blue) and +0.40 (red) during two cycles on the asymmetrical side of the transition boundary for a self-propelled plunging rigid rectangular plate with $\delta = 0.1$, at (a) at $KC = 3.8$ and $\beta = 10.4$; (b) at $KC = 4.2$ and $\beta = 8.33$ 74

Figure 22. Variation of transition boundaries allowing horizontal motion in KC - β space along with power curve fitting for varying δ ($0.05 \leq \delta \leq 0.2$) . Region (i) represents no horizontal motion, region (ii) represents conditional horizontal motion and region (iii) represents unhindered horizontal motion..... 75

Figure 23. Variation of Floquet multiplier with KC at $\beta = 59.52$ for $\delta = 0.1$ 78

Figure 24. Non-dimensionalized trajectory coordinate (X) of the centre of mass of the self-propelled plunging plate as a function of flapping cycles (t/T) with $\delta = 0.1$ for $\beta = 60$ and $KC = 1.2$, and $\beta = 60$ and $KC = 1.5$ 78

Figure 25. Fifteen evenly spaced contours between -0.40 (blue) and +0.40 (red) of periodic base flow at $\beta = 60.0$ for $\delta = 0.1$ (a) vorticity at $KC = 1.2$. (b) eigenvector at $KC = 1.2$, (c) vorticity at $KC = 1.5$, and (d) eigenvector at $KC = 1.5$ 80

Figure 26. (a) dimensional trajectory coordinate (X) for $\delta = 0.05$ of center of mass at (1) $KC = 1.2$ and $\beta = 83.33$, (2) $KC = 1.8$ and $\beta = 41.67$, (3) $KC = 2.4$ and $\beta = 20.8$ and (4) $KC = 4.2$ and $\beta = 8.33$ with flapping cycles. (b) Location of transition boundary as a function of KC - β with cases marked as (1), (2), (3) and (4)..... 81

Figure 27 (a,b,c). wake patterns associated with plunging flat plate for cases (1), (2), (3) and (4). The right column shows the instantaneous positions and trajectory during one cycle. Red

and blue colors indicate anti-clockwise and clockwise rotation respectively. The white arrows show the direction of horizontal movement of the plate.....83

Figure 28. (a) Time variation of horizontal thrust for cases (1), (2), (3), and (4). (b) Phase portraits plotting the time rate of change dC_x/dt of the horizontal thrust against C_x for the same cases (i.e. (1), (2), (3), and (4)).84

Figure 29. A self-propelled plunging rigid plate for $\delta=0.05$ corresponding to cases (1), (2), (3) and (4) (a) Time dependence of horizontal thrust. (b) Horizontal thrust power spectra.85

Figure 30. The non-dimensional trajectory coordinate (X) of the center of mass of self-propelled plunging plate as a function of time for $\delta=0.05$ at $KC=1.8$ and $\beta=41.67$ with different ground clearances.....86

Figure 31. (a) A schematic representation of rectangular boxes ($4D \times 3D$) around the plate for calculating the circulation. (b) The variation of non-dimensional circulation ($|I|$) as a function of ground clearance (ζ) with $\delta=0.05$ at $KC=1.8$ and $\beta=41.67$ at $t/T=30$, when the instantaneous position at maximum displacement during the upstroke.87

LIST OF TABLES

Table 1. Features of prior research on the self-propelled rigid flapping membrane.....	18
Table 2. Highlights of some earlier studies on linear stability analysis.....	22
Table 3 Highlights of few earlier studies on Floquet analysis.....	26
Table 4. Global count representation of all the points on the grid with appropriate neighbors.	48
Table 5. The complex conjugate eigenvalues with the smallest real part of flow past a square cylinder at $Re = 45.0$	53
Table 6. Comparison of results for unsteady two-dimensional flow past a stationary square cylinder for $Re = 100$	54
Table 7. Strouhal-Reynolds number variation obtained in present simulation and compared with Sen et al. [119] for $60 \leq Re \leq 100$	54
Table 8. The complex conjugate eigenvalues with the smallest real part for the double-glazing problem at $Ra = 1.5 \times 10^6$	60
Table 9. The complex conjugate eigenvalues with the smallest real part for the double-glazing problem for Ra from 1.5×10^6 to 2.0×10^6	60
Table 10. The scope of parameters (or configuration space) examined in this work for the parametric study of a rigid plunging plate.	68
Table 11. Values of a_0 , a_1 , b_0 , and b_1 for varying δ corresponding to Eq. (5.6) and Eq. (5.7). 76	

NOMENCLATURE

a	length of a side of the solid cylinder
A	plunging amplitude
B	blockage ratio of the domain
\mathbf{B}	discrete velocity space
c	unit lattice speed
c_s	speed of sound
C_x	thrust coefficient
D	chord length
\mathbf{e}_i	discrete velocity vector
E_k	kinetic energy
f	vortex shedding frequency
f_o	primary oscillation frequency
f_i	particle velocity distribution function
f_i	post collision distribution function (SRT)
f_i^{eq}	equilibrium velocity distribution function
f	moments of a distribution function
f_*	post collision distribution function (MRT)
\bar{F}_x	instantaneous dimensional thrust
g	acceleration due to gravity
g_i	energy distribution function
g_i^{eq}	equilibrium energy distribution function

h	domain height
J	Jacobian matrix
KC	Keulegan-Carpenter number
M	mass matrix
Z	transformation matrix
N	grid points
p	pressure
Q	Moment space
Pr	Prandtl number
Ra	Rayleigh number
Re	Reynolds number
Re_c	Critical Reynolds number
Re_f	flapping Reynolds number
Re_{fc}	Critical plunging Reynolds number
Re_u	translational Reynolds number
S	Diagonal relaxation time matrix
s_i	viscous heat dissipation
S_L	length scale
St	Strouhal number
S_T	temperature scale
\tilde{t}	characteristic timescale
t	time
T	duration of one cycle
u	the instantaneous translational velocity of foil
\mathbf{u}	the velocity vector of the fluid

u_{dipole}	velocity of dipoles
\bar{u}	time-averaged translational velocity
U_∞	free-stream velocity
w_i	weighing factor
x	eigenfunction
X	the position vector of the centre of mass
y	plunging displacement

Greek Symbols

β	Stokes number
β_c	Critical Stokes number
ζ	ground clearance
δ	Thickness to chord ratio
κ	coefficient of volumetric expansion
ν	kinematic viscosity of the fluid
ρ_f	the density of the fluid
ρ_s	the density of the solid
ρ^*	Density ratio
σ	complex growth rate
τ_f	dimensionless relaxation time for LBE
τ_g	dimensionless relaxation time for TLBE
ϕ_i	accounts for any external forces acting on a fluid
χ	thermal diffusivity
ψ	stream function
ω	vorticity transport

Γ circulation

ξ the separation between vortex centres

Ω Collision operator